

## Supporting Information

# **pH-Responsive lower critical solution temperature behaviour of a dibenzo-24-crown-8 based low-molecular- weight gelator in water**

Bo Zheng,<sup>a</sup> Huizheng Zhang,<sup>a</sup> Na Wang<sup>a</sup> and Lingyan Gao<sup>\*a</sup>

*a Key Laboratory of Synthetic and Natural Functional Molecule Chemistry of the Ministry of Education,  
College of Chemistry and Materials Science, Northwest University, Xi'an 710069, P. R. China. E-mail:  
[gaolingyan@nwu.edu.cn](mailto:gaolingyan@nwu.edu.cn)*

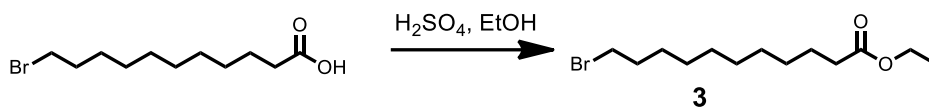
## Table of Contents

1.	Materials and methods	S3
2.	Synthesis of gelator <b>1</b>	S3
3.	Scanning electron microscopy of <b>1•K</b>	S10
4.	Transmission electron microscopy of <b>1•K</b>	S11
5.	LCST phase transition behavior of <b>1•K</b> in water solution	S12
6.	Acid-base controlled thermo-responsiveness of <b>1•K</b>	S13
7.	Atomic force microscopy of <b>1•K</b>	S13
	reference	S15

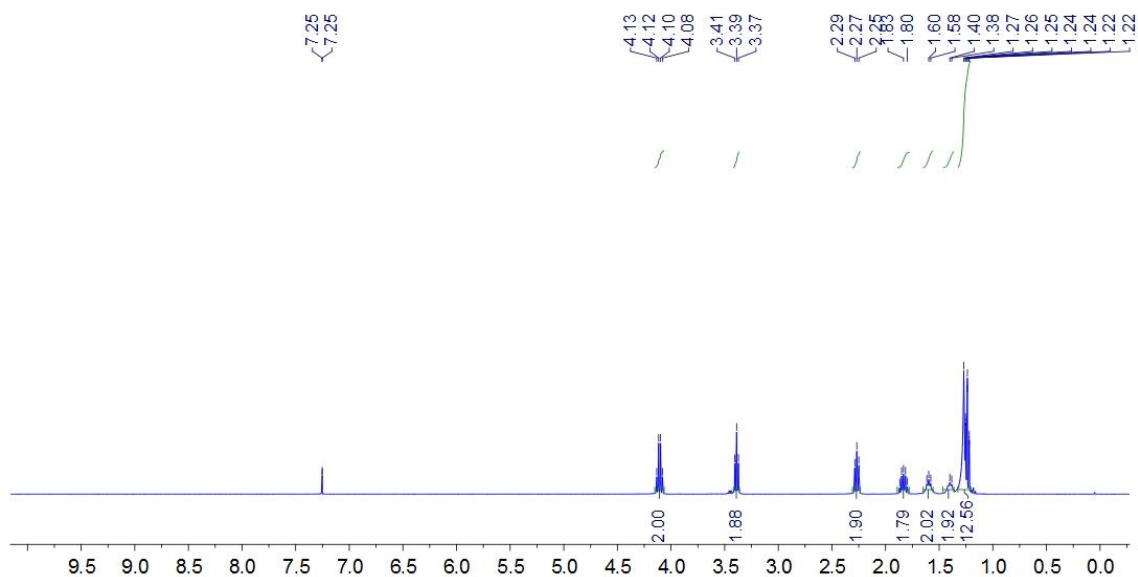
## 1. Materials and methods

All reagents were commercially available and used as supplied without further purification. KOH is purchased from Acros (99.98%). Sodium hydroxide solution (0.1 N) and Potassium hydroxide solution (0.1N) are from Titripur® Merck, Titripur® Merck, while HCl (0.1 N) is from Titripur® Reag. Ph Eur, Reag. USP. NMR spectra were recorded with a Bruker 700 MHz spectrometer, a Bruker Avance III 500 spectrometer, or a Bruker Avance III-400 spectrometer using the deuterated solvent as the lock and the residual solvent or TMS as the internal reference. The transmittance experiments were measured at 550 nm (5 mm cuvette) using a Lambda 950 UV/Vis/NIR spectrometer with a temperature control system. The heating rate was adjusted at 1.0 °C/min. Dynamic light scattering (DLS) was used to measure the hydrodynamic size of the particles as a function of temperature in a 20–80 °C range on a Malvern Zetasizer Nano ZS with a diode laser at 90° of scattering angle, a wavelength at 633 nm, and a power of 15 mW. Unless otherwise stated, samples were dispersed in Milli-Q water.

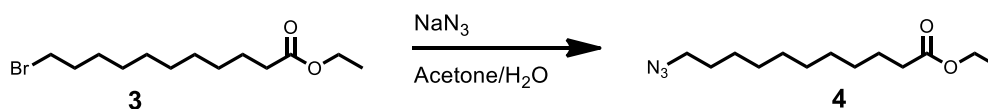
## 2. Synthesis of gelator 1



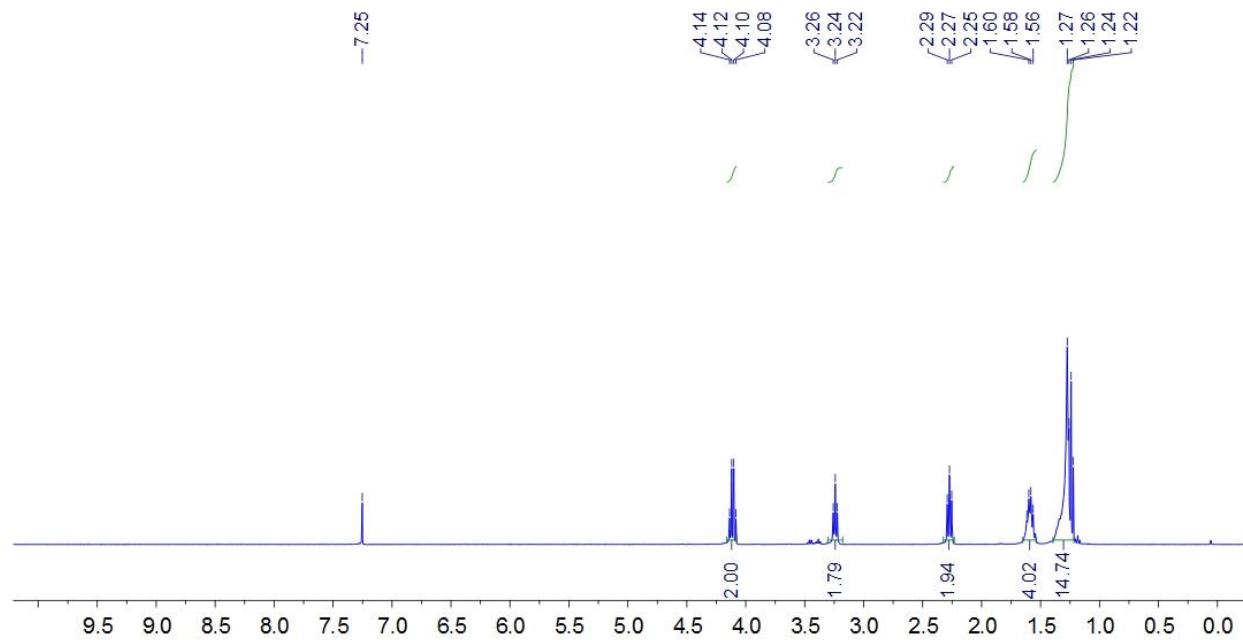
11-Bromoundecanoic acid (4.60 g, 17.40 mmol) was dissolved in ethanol (35 mL) and 3 mL of H<sub>2</sub>SO<sub>4</sub> was added dropwise to the ethanol solution.<sup>S1</sup> The mixture solution was heated under reflux overnight. It was allowed to cool down, and the solvents were evaporated. The resulted residue was dissolved in ethyl acetate (EtOAc) and washed with brine. The organic layer was dried over MgSO<sub>4</sub>, and evaporated to give an oily compound **3** (4.69 g, yield: 92%). The proton NMR spectrum of **3** is shown in Figure S1. <sup>1</sup>H NMR (400 MHz, CDCl<sub>3</sub>, 295K)  $\delta$  (ppm): 4.11 (q,  $J = 7.2$  Hz, 2H), 3.39 (t,  $J = 6.9$  Hz, 2H), 2.27 (t,  $J = 7.5$  Hz, 2H), 1.89 – 1.78 (m, 2H), 1.65 – 1.56 (m, 2H), 1.44 – 1.36 (m, 2H), 1.33 – 1.25 (m, 10H), 1.24 (t,  $J = 7.2$  Hz, 3H).



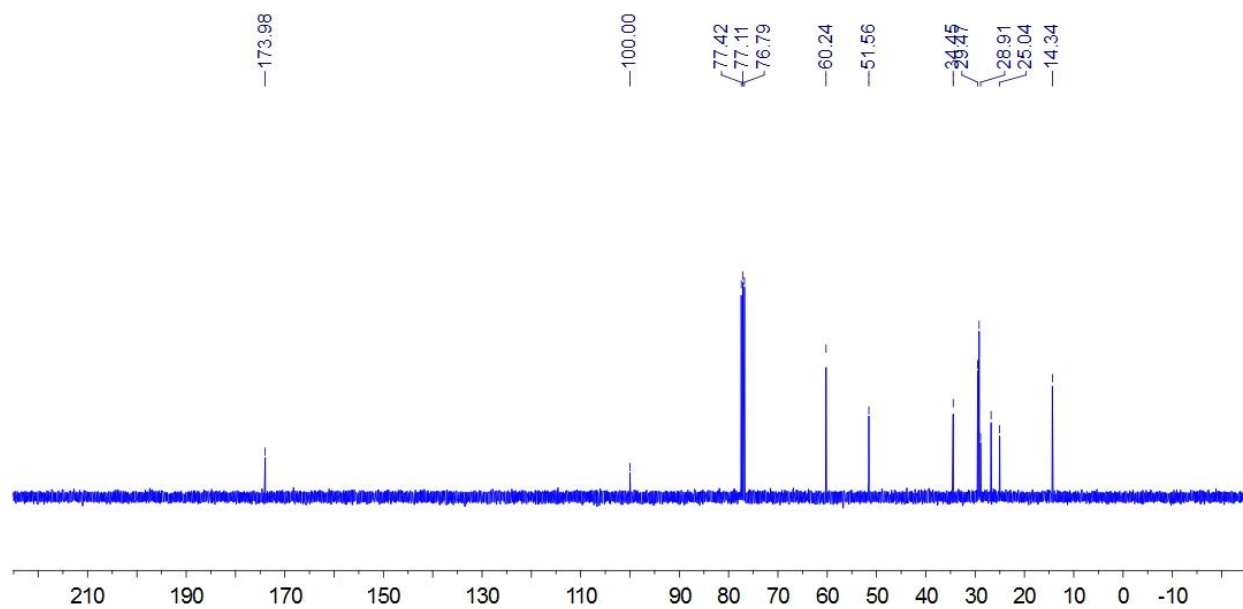
**Figure S1.**  $^1\text{H}$  NMR spectrum (400 MHz,  $\text{CDCl}_3$ , 295K) of **3**.



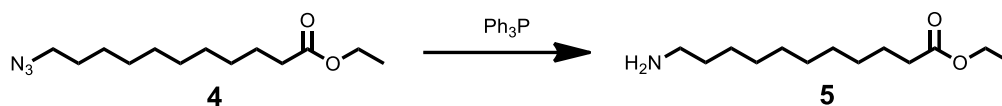
**3** (1.31 g, 4.50 mmol) and sodium azide (0.29 g, 4.50 mmol) were dissolved in the mixture solution of acetone (50 mL) and  $\text{H}_2\text{O}$  (5 mL). After refluxing for 36 h, acetone was evaporated under reduced pressure, and the solution was extracted with  $\text{CH}_2\text{Cl}_2$ . The organic layers were combined, washed with water and brine, and then dried over  $\text{MgSO}_4$ . The solvent was evaporated to afford oily **4** (1.04 g, 91%). The proton NMR spectrum of **4** is shown in Figure S2.  $^1\text{H}$  NMR (400 MHz,  $\text{CDCl}_3$ , 295K)  $\delta$  (ppm): 4.11 (q,  $J = 7.2$  Hz, 2H), 3.24 (t,  $J = 7.0$  Hz, 2H), 2.27 (t,  $J = 7.5$  Hz, 2H), 1.65 – 1.53 (m, 4H), 1.38 – 1.25 (m, 12H), 1.24 (t,  $J = 7.2$  Hz, 3H). The  $^{13}\text{C}$  NMR spectrum of **4** is shown in Figure S3.  $^{13}\text{C}$  NMR (100 MHz,  $\text{CDCl}_3$ , 295 K)  $\delta$  (ppm): 173.98, 100.00, 60.24, 51.56, 34.45, 29.47, 29.39, 29.29, 29.19, 28.91, 26.78, 25.04, 14.34. HRESIMS:  $m/z$  calcd for  $[\text{M}+\text{Na}]^+$   $\text{C}_{13}\text{H}_{25}\text{N}_3\text{NaO}_2$ , 278.1839; found 278.1839, error 0 ppm.



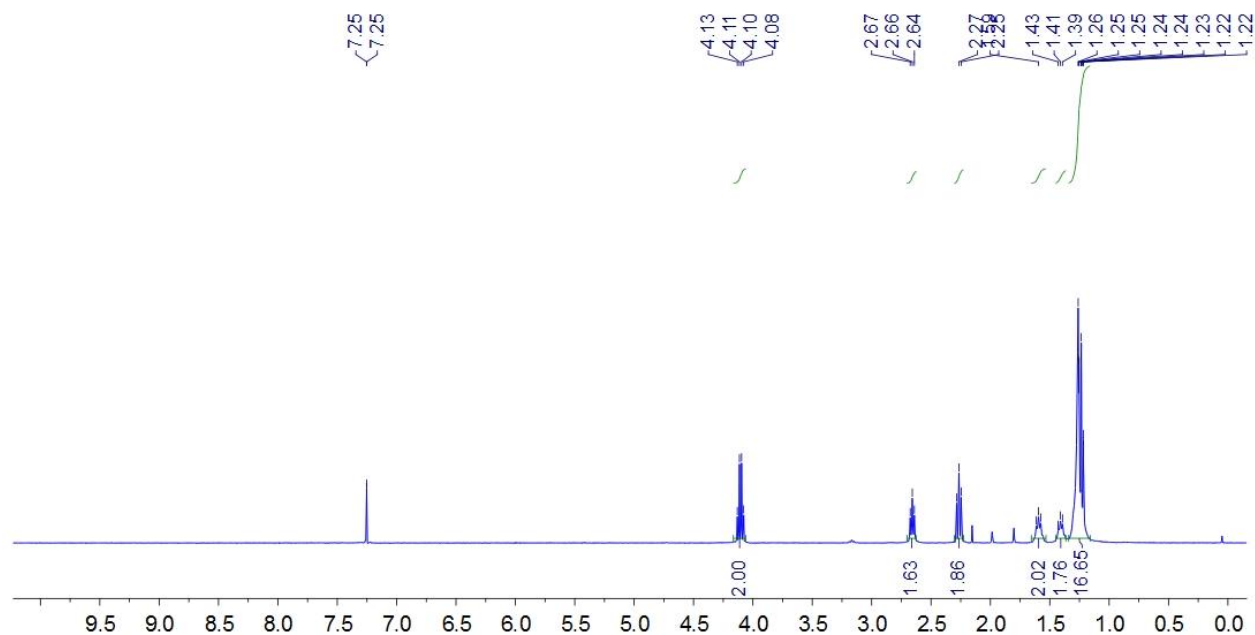
**Figure S2.**  $^1\text{H}$  NMR spectrum (400 MHz,  $\text{CDCl}_3$ , 295K) of **4**.



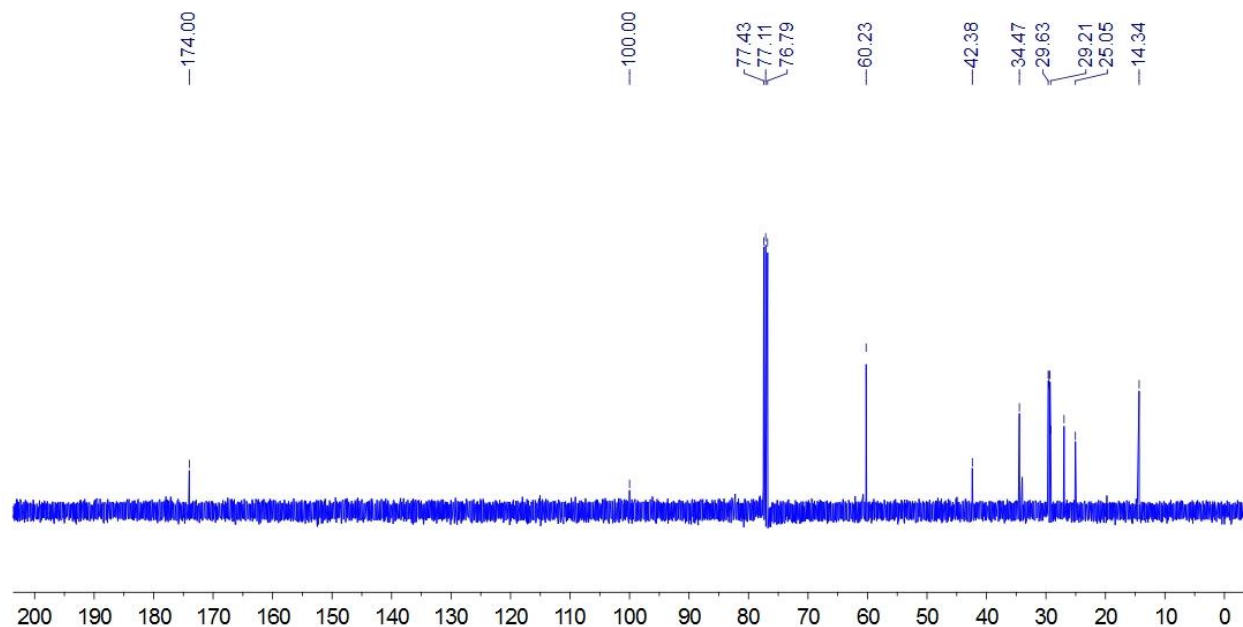
**Figure S3.**  $^{13}\text{C}$  NMR spectrum (100 MHz,  $\text{CDCl}_3$ , 295K) of **4**.



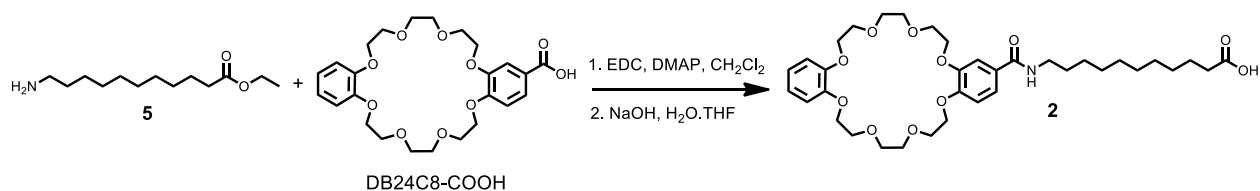
Ph<sub>3</sub>P (0.86 g, 3.30 mmol) was added to a solution of **4** (0.42 g, 1.70 mmol) (20 mL of THF and 2 mL of H<sub>2</sub>O). After stirred for 2 days, THF was removed under reduced pressure. The residue was dissolved in CH<sub>2</sub>Cl<sub>2</sub>, and washed twice with diluted HCl. The acidic aqueous phases were combined and extracted with EtOAc. Then, the pH of the aqueous phase was carefully adjusted to ~10. The resulted solution was extracted with CH<sub>2</sub>Cl<sub>2</sub>, and the collected organic layers were dried over MgSO<sub>4</sub>. The solvent was evaporated to afford oily **5** (0.26 g, 69%). The proton NMR spectrum of **5** is shown in Figure S4. <sup>1</sup>H NMR (400 MHz, CDCl<sub>3</sub>, 295K) δ (ppm): 4.10 (q, *J* = 7.2 Hz, 2H), 2.66 (t, *J* = 7.0 Hz, 2H), 2.27 (t, *J* = 7.5 Hz, 2H), 1.64 – 1.54 (m, 2H), 1.45 – 1.36 (m, 2H), 1.34 – 1.24 (m, 12H), 1.24 (t, *J* = 7.2 Hz, 3H). The <sup>13</sup>C NMR spectrum of **5** is shown in Figure S5. <sup>13</sup>C NMR (100 MHz, CDCl<sub>3</sub>, 295 K) δ (ppm): 174.00, 100.00, 60.23, 42.38, 34.47, 29.63, 29.55, 29.47, 29.32, 29.21, 26.96, 25.05, 14.34. HRESIMS: *m/z* calcd for [M+H]<sup>+</sup> C<sub>13</sub>H<sub>28</sub>NO<sub>2</sub>, 230.2115; found 230.2121, error 2.6 ppm.



**Figure S4.** <sup>1</sup>H NMR spectrum (400 MHz, CDCl<sub>3</sub>, 295K) of **5**.



**Figure S5.**  $^{13}\text{C}$  NMR spectrum (100 MHz,  $\text{CDCl}_3$ , 295K) of **5**.



A mixed solution of **5** (300 mg, 1.31 mmol), DB24C8-COOH (644 mg, 1.31 mmol), EDC (392 g, 2.00 mmol) and DMAP (15 mg, 0.12 mmol) in dichloromethane (DCM, 10 mL) was stirred for two days at room temperature. Then, the solvent was removed to give a crude product, which was subjected to column chromatography (DCM : MeOH = 10 : 1) to remove undesired side products. To a solution of the intermediate product (400 mg, 0.58 mmol) in 15 mL of THF and 15 mL of  $\text{H}_2\text{O}$  was added sodium hydroxide (232 mg, 5.80 mmol). The solution stirred at room temperature for 3 h. After removal of THF, HCl was added to protonate the compound and white precipitate formed. The precipitate was filtered, collected and dried to give compound **2** as a white solid (350 mg, 90%). The proton NMR spectrum of **2** is shown in Figure S6.  $^1\text{H}$  NMR (700 MHz,  $\text{DMSO}-d_6$ , 295K)  $\delta$ (ppm): 11.89 (br, 1H), 8.25 (t,  $J = 5.6$  Hz, 1H), 7.43 (d,  $J = 8.4$ , 1H), 7.42 (s, 1H), 6.99 (d,  $J = 8.4$ , 1H), 6.95 – 6.92 (m, 2H), 6.88 – 6.85 (m, 2H), 4.13 – 4.09 (m, 4H), 4.07 – 4.04 (m, 4H), 3.79 – 3.74 (m, 8H), 3.68 – 3.65 (m, 8H), 3.21 (t,  $J = 6.7$ , 2H), 2.17 (t,  $J = 7.4$ , 2H), 1.51 – 1.45 (m, 4H), 1.30 – 1.22 (m, 12H). The  $^{13}\text{C}$  NMR spectrum of **2** is shown in Figure S7.  $^{13}\text{C}$  NMR (175 MHz,  $\text{DMSO}-d_6$ , 295 K)  $\delta$  (ppm): 174.94, 165.89, 165.82, 151.17, 148.94, 148.11, 127.71, 127.67, 121.14, 114.58, 114.53, 113.08, 112.96, 70.93, 70.89, 70.86, 69.63, 69.54, 69.47, 69.35, 69.18, 34.13, 29.67, 29.40, 29.33, 29.24, 29.19, 29.01, 26.98, 24.93. HRESIMS:  $m/z$  calcd for  $[\text{M}+\text{K}]^+$   $\text{C}_{36}\text{H}_{53}\text{KNO}_{11}$ , 714.3250; found 714.3256, error 0.8 ppm.

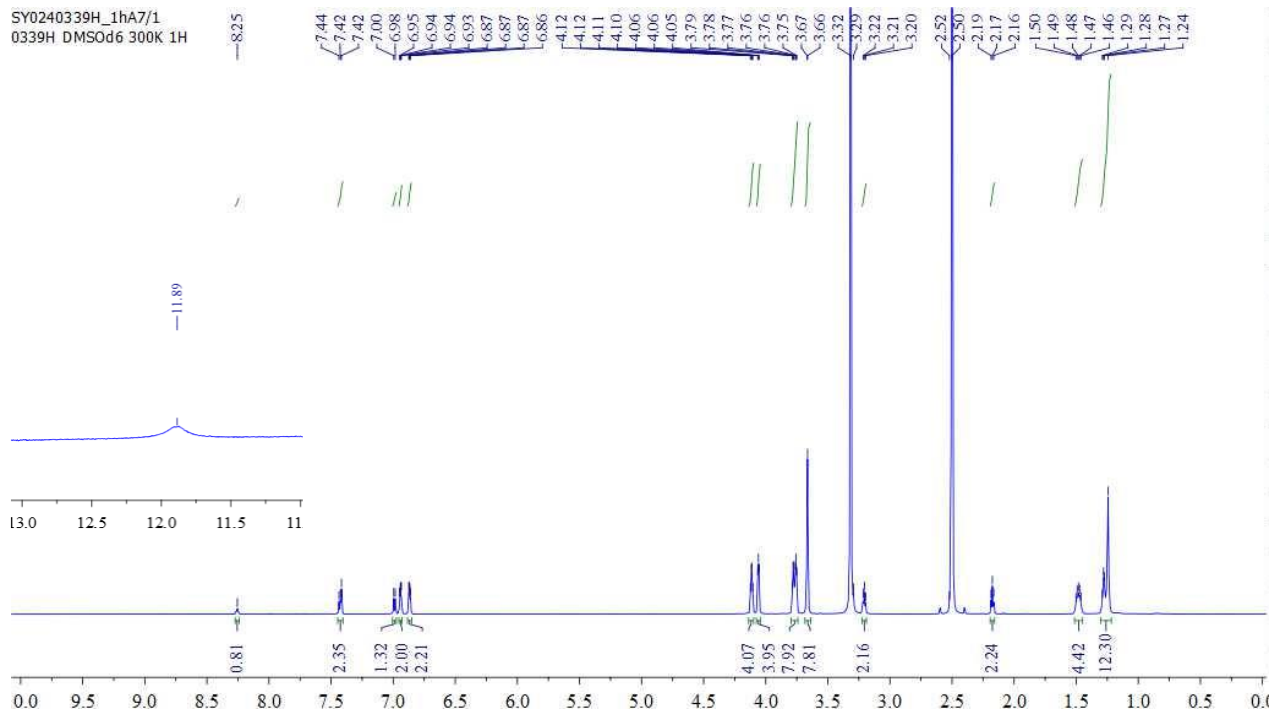


Figure S6.  $^1\text{H}$  NMR spectrum (700 MHz,  $\text{DMSO-}d_6$ , 295K) of **2**.

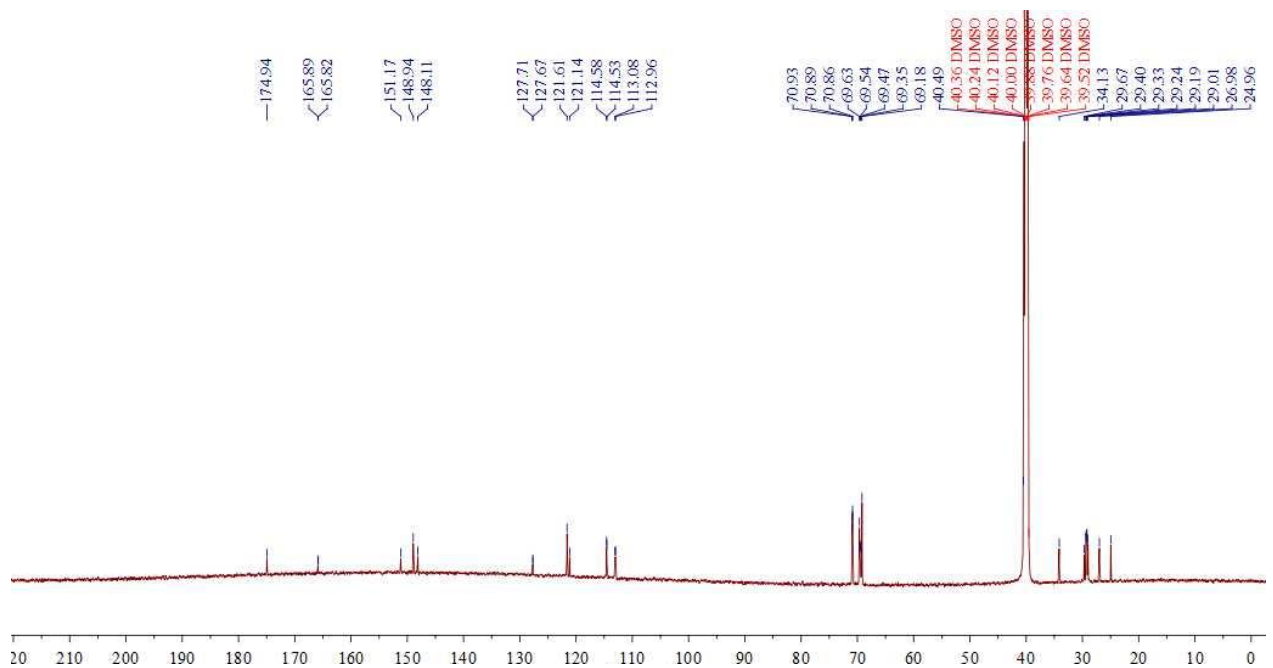
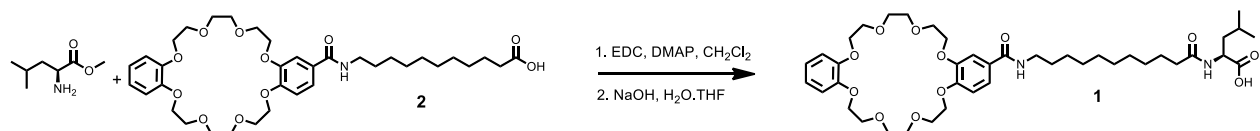
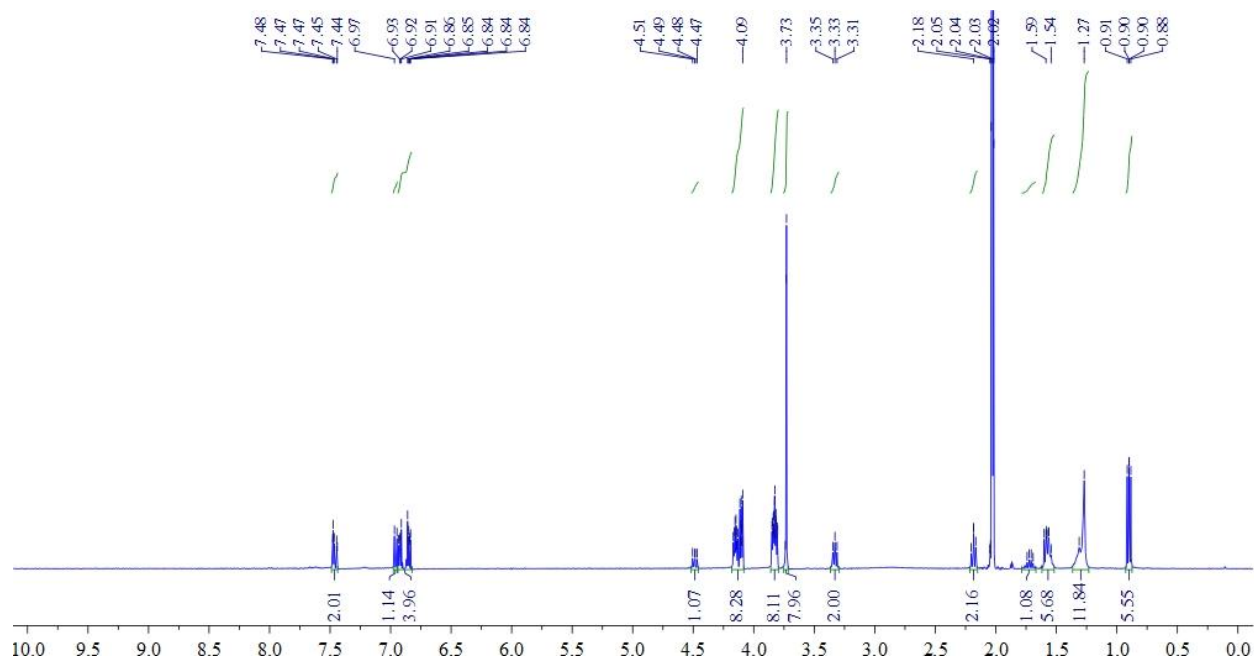


Figure S7.  $^{13}\text{C}$  NMR spectrum (175 MHz,  $\text{DMSO-}d_6$ , 295K) of **2**.

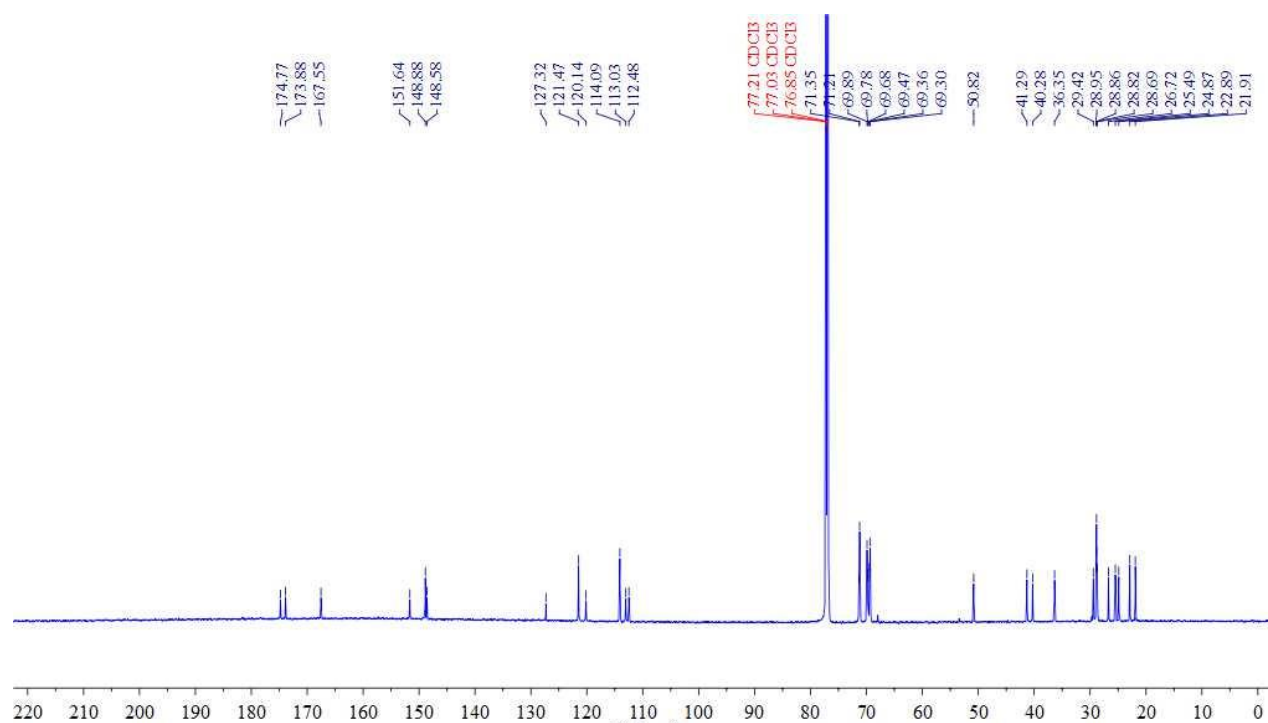




A solution of **2** (41 mg, 0.06 mmol), L-Leu-OMe-HCl (24 mg, 0.13 mmol), EDC (25 mg, 0.13 mmol) and DMAP (17 mg, 0.14 mmol) in dichloromethane (5 mL) was stirred for two days at room temperature. The solvent was removed to give a crude product, which was subjected to column chromatography (DCM : MeOH = 20 : 1) to obtain the pure intermediate product as an solid. To a solution of that (38 mg, 0.05 mmol) in 5 mL of THF and 5 mL of H<sub>2</sub>O was added sodium hydroxide (8 mg, 0.20 mmol). The solution was stirred at 45 °C for 3 h. After removal of THF, 1M HCl (1 mL) was added to protonate the compound and white precipitate formed. The precipitate was filtered, collected and dried to give compound **1** as a white solid (33 mg, 89%). The proton NMR spectrum of **1** is shown in Figure S8. <sup>1</sup>H NMR (400 MHz, acetone-*d*<sub>6</sub>, 295K)  $\delta$  (ppm): 7.48 (d, *J* = 2.0, 1H), 7.47 – 7.44 (m, 1H), 6.96 (d, *J* = 8.3, 1H), 6.94 – 6.90 (m, 2H), 6.87 – 6.82 (m, 2H), 4.49 (m, 1H), 4.18 – 4.13 (m, 4H), 4.13 – 4.09 (m, 4H), 3.86 – 3.80 (m, 8H), 3.75 – 3.71 (m, 8H), 3.33 (t, *J* = 7.1, 2H), 2.18 (d, *J* = 7.0, 2H), 1.72 (m, 1H), 1.62 – 1.53 (m, 6H), 1.37 – 1.23 (m, 12 H), 0.90 (dd, *J* = 6.6, 5.4, 6H). The <sup>13</sup>C NMR spectrum of **1** is shown in Figure S9. <sup>13</sup>C NMR (175 MHz, CDCl<sub>3</sub>, 295 K)  $\delta$  (ppm): 174.77, 173.88, 167.55, 151.64, 148.88, 148.58, 127.32, 120.14, 114.09, 113.03, 112.48, 71.35, 71.21, 69.89, 69.78, 69.68, 69.47, 69.36, 69.30, 50.82, 41.29, 40.28, 36.35, 29.42, 28.95, 28.86, 28.82, 28.69, 26.72, 25.49, 24.87, 22.89, 21.91. HRESIMS: *m/z* calcd for [M+Na]<sup>+</sup> C<sub>42</sub>H<sub>64</sub>N<sub>2</sub>NaO<sub>12</sub>, 811.4351; found 811.4383, error 3.9 ppm.

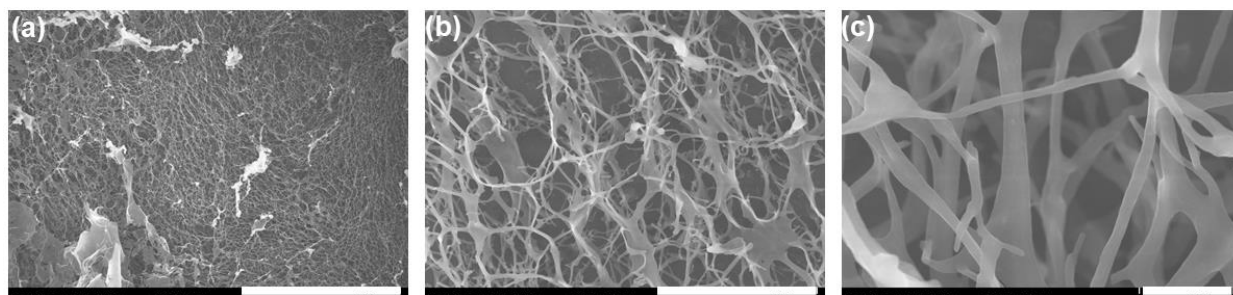


**Figure S8.** <sup>1</sup>H NMR spectrum (400 MHz, acetone-*d*<sub>6</sub>, 295K) of **1**.



**Figure S9.**  $^{13}\text{C}$  NMR spectrum (175 MHz,  $\text{CDCl}_3$ , 295K) of **1**.

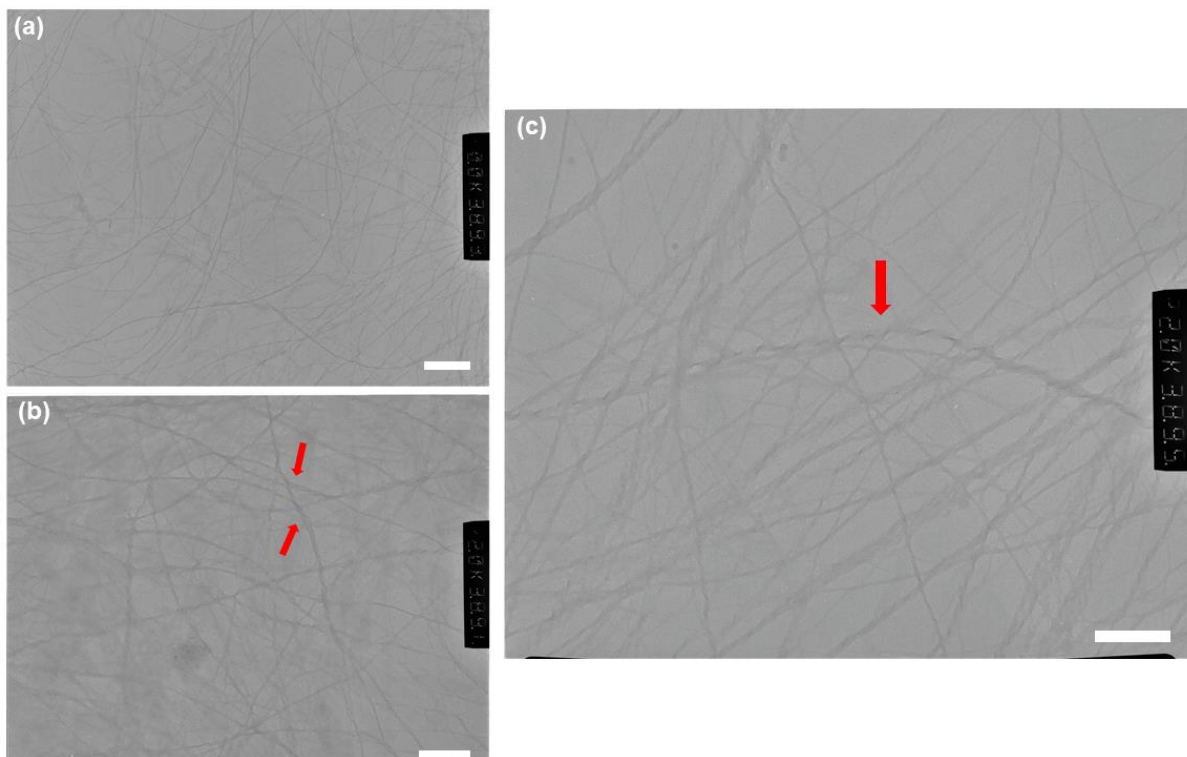
### 3. Scanning electron microscopy of **1**·**K**



**Figure S10.** SEM images of the xerogel (**1**·**K**<sub>1.0</sub>, 0.9 wt%), scale bar: 100  $\mu\text{m}$  (a), 10  $\mu\text{m}$  (b), and 1  $\mu\text{m}$  (c).

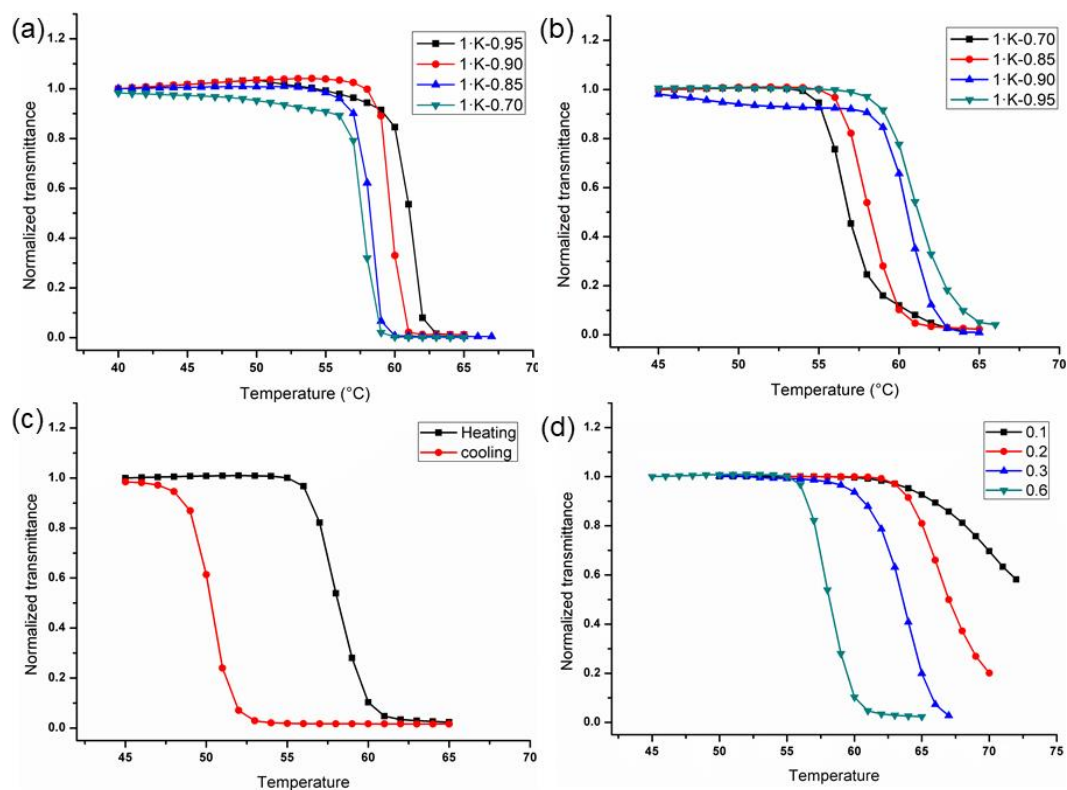
The entanglement of long ribbons of **1**·**K**<sub>1.0</sub> forms a fibrous gel network.

#### 4. Transmission electron microscopy of $1\cdot\mathbf{K}$



**Figure S11.** TEM images of the gel ( $1\cdot\mathbf{K}_{1.0}$ , 0.1 wt%), scale bar: 1  $\mu\text{m}$  (a), 0.45  $\mu\text{m}$  (b), and 0.45  $\mu\text{m}$  (c). The low concentration solution of  $1\cdot\mathbf{K}_{1.0}$  forms long thin helical fibrils, which can be observed in these images. When the concentration of the gelator increases, these smaller fibrils would further assemble to form stronger ribbons to be the backbone of the hydrogel network.

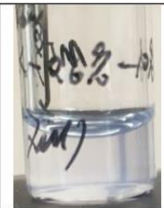

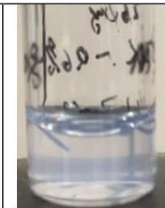
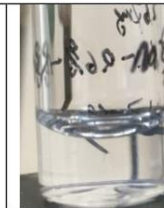

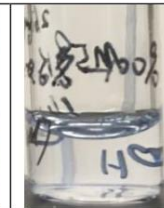
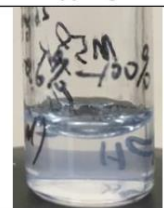



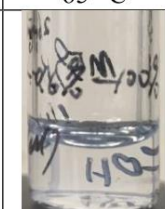
## 5. LCST phase transition behavior of $1\cdot K$ in water solution



**Figure S12.** Temperature-dependence of light transmittance of: (a)  $1\cdot K_x$  (1.2 wt%,  $x = 0.70, 0.85, 0.90$  and  $0.95$ ) measured at 550 nm; (b)  $1\cdot K_x$  (0.6 wt%,  $x = 0.70, 0.85, 0.90$  and  $0.95$ ); (c) heating-cooling cycle of  $1\cdot K_{0.85}$  (0.6 wt%); (d)  $1\cdot K_{0.85}$  at 0.6 wt%, 0.3 wt%, 0.2 wt% and 0.1 wt%.

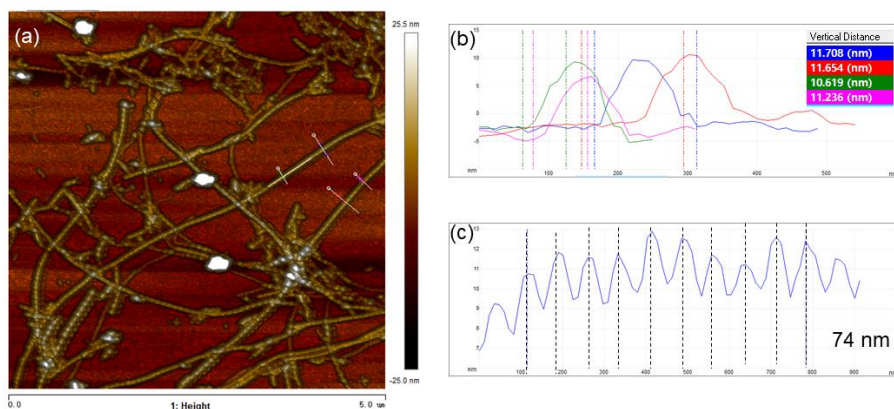
Both  $1\cdot K_x$  at 1.2 wt% and 0.6 wt% show the same trend that with the larger  $x$ , the  $T_{\text{cloud}}$  increases correspondingly. Considering the importance of the deprotonation ratio of the carboxyl group on **1** for its LCST behaviour, both **1** with charged and neutral states in the solution are crucial for the LCST behaviour. The co-existing neutral and charged carboxyl groups in  $1\cdot K_{0.85}$ , for example, can result in different hydrogen bonding pattern and self-assembly process. The spontaneous co-assembly process between the deprotonated monomer **1** and remaining neutral form can be affected in response to a change in temperature. Sample  $1\cdot K_{0.85}$  exhibits very shape transition in the heating process and show a hysteresis in the following cooling process (less than 10 °C). The further dilution of  $1\cdot K_{0.85}$  results in the higher transition temperatures.

## 6. Acid-base controlled thermo-responsiveness of $1\cdot K$

			→			
x = 0.70, r.t.	x = 0.70, 65 °C	x = 0.70, cool down to r.t.	KOH	x = 1.0, r.t.	x = 1.0, 65 °C	x = 1.0, cool down to r.t.
→			...	→		...
HCl	x = 0.70, r.t.	x = 0.70, 65 °C	...	KOH	x = 1.0, 65 °C	...
→						
HCl	x = 0.70, 65 °C	x = 0.70, cool down to r.t.				

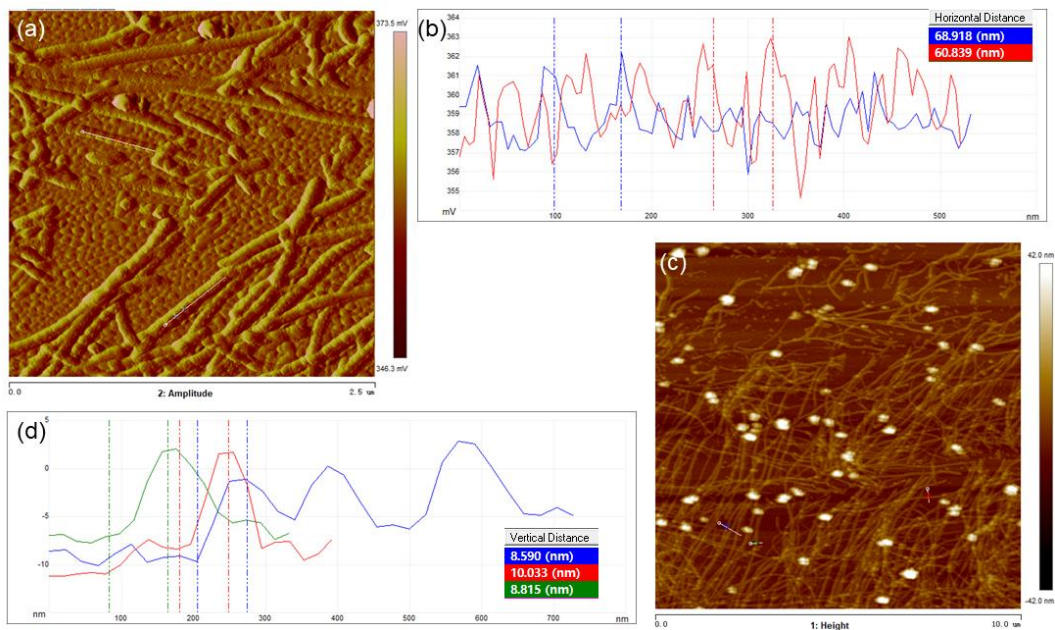
**Figure S13.** A  $1\cdot K_x$  sample at 0.6 wt% was prepared and the deprotonation ratio  $x$  was adjusted by the consecutive addition of acid (HCl) or base (KOH), leading to the off/on switch of LCST.

## 7. Atomic force microscopy of $1\cdot K$

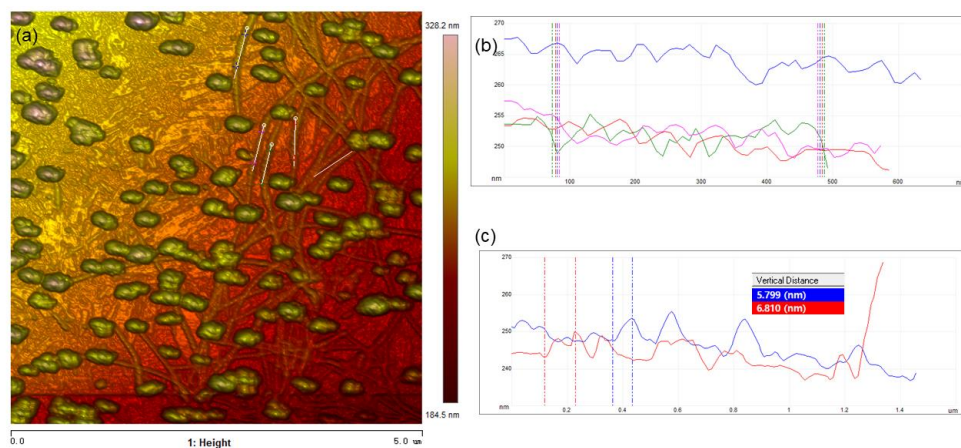


**Figure S14.** (a) AFM image of  $1\cdot K_{1.0}$  (0.06 wt%) with long helical fibrils, scale:  $5\ \mu\text{m} \times 5\ \mu\text{m}$ ; (b) height profiles across two fibrils of ca. 11.3 nm and (c) along a fibril with 74 nm helical pitch in (a).





**Figure S15.** (a) AFM image of  $1 \cdot K_{0.95}$  (0.06 wt%), scale:  $2.5 \mu\text{m} \times 2.5 \mu\text{m}$ ; (b) helical pitches along a fibril in (a); (c) AFM image of  $1 \cdot K_{0.95}$  (0.06 wt%) with long helical fibrils and particles, scale:  $10 \mu\text{m} \times 10 \mu\text{m}$ ; and (d) height profiles across three fibrils in (c).



**Figure S16.** (a) AFM image of  $1 \cdot K_{0.85}$  (0.06 wt%) with long helical fibrils and particles, scale:  $5 \mu\text{m} \times 5 \mu\text{m}$ ; (b) helical pitches along a fibril and (c) height profiles across two fibrils in (a). Helical pitches and height profiles reveal a less uniform fibril structure of  $1 \cdot K_{0.85}$ .

Reference:

S1. Y. Zhou, W. Pei, X. Zhang, W. Chen, J. Wu, C. Yao, L. Huang, H. Zhang, W. Huang, J. S. C Loo and Q. Zhang, *Biomaterials*, 2015, **54**, 34-43.